



CHORUS

This is the accepted manuscript made available via CHORUS. The article has been published as:

X-Ray Parametric Down-Conversion in the Langevin Regime

S. Schwartz, R. N. Coffee, J. M. Feldkamp, Y. Feng, J. B. Hastings, G. Y. Yin, and S. E. Harris

Phys. Rev. Lett. **109**, 013602 — Published 6 July 2012

DOI: [10.1103/PhysRevLett.109.013602](https://doi.org/10.1103/PhysRevLett.109.013602)

X-ray Parametric Down-Conversion in the Langevin Regime

S. Shwartz,^{1,*} R. N. Coffee,² J. M. Feldkamp,² Y. Feng,² J. B. Hastings,² G. Y. Yin,¹ and S. E. Harris¹

¹*Edward L. Ginzton Laboratory, Stanford University, Stanford, California 94305*

²*The Linac Coherent Light Source, SLAC National Accelerator Laboratory, Menlo Park, California 94025, USA*

We experimentally and theoretically study the coincidence count rate for down-converted x-ray photons. Because of photoionization, parametric down-conversion at x-ray wavelengths generally involves loss and the theoretical description requires a Langevin approach. By working in a transmission geometry (Laue) rather than in the Bragg geometry of previous experiments we obtain an improvement in the signal to noise ratio of 12.5, and find agreement between experiment and theory.

PACS numbers: 42.65.Lm 42.50.Ct 05.10.Gg

For decades parametric down-conversion (PDC) has been widely used as a source for generating entangled photons in the infrared and visible spectral regimes, and has resulted in remarkable insights into many quantum phenomena [1]. The extension of PDC to the x-ray regime was proposed by Freund [2] and demonstrated with a hard-x-ray tube by Eisenberger forty years ago [3]. The essence of these early papers was the realization that though the plasma-like nonlinearity at x-ray wavelengths is much smaller than visible nonlinearities, the number of driving k-space modes is vastly larger. In recent years the use of synchrotrons has allowed considerable experimental progress [4], and recent experiments have opened the possibility for investigating the optical response of chemical bonds by PDC from the x-ray to the x-ray and UV range [5–7]. New theoretical results suggest a method for generating Bell states at x-ray wavelengths [8], thereby allowing the possibility of the use of high efficiency photon number state resolving detectors.

This Letter describes a substantial difference between PDC as observed in the visible and at x-ray wavelengths. This difference is the result of the inherent loss due to photoionization at the generated x-ray wavelengths, as compared to the near zero loss at generated optical and infrared wavelengths. For example, the absorption coefficient of diamond at 4 keV is 132.6 cm^{-1} and at 9 keV is 10.2 cm^{-1} . Theories [9, 10] that are correct when there is no loss are incorrect in the presence of loss. In the Heisenberg picture, without loss, vacuum fields at the signal and idler at the crystal input act as the driver for the down-conversion process. In the presence of loss these vacuum fields decay and a non-Langevin theory predicts that the parametric fluorescence exponentially approaches zero as the crystal length becomes many decay lengths long. This shortcoming is removed by the inclusion of appropriate Langevin terms in the Heisenberg equation. In this picture the loss process at the signal or idler is inherently tied to fluctuation, and these fluctuations are the driver for the down-conversion process. This is far more than a technical correction: with the Langevin fluctuations included, the signal and idler count rates, as well as the coincidence count rate, for a

sufficiently long crystal, depend on the absorption length but not on the crystal length.

The previous theory of x-ray PDC [2] relies on the early work of Kleinman [10]. It describes the count rate of a single detector measuring one of the paired photons, while all experimental x-ray down-conversion papers have described coincidence count rates. In the presence of loss, the coincidence count rate is substantially lower than the single photon count rate. For example, our calculations show that when the pump photon energy is 18 keV, and the photon energy of the signal and the idler photons is 9 keV, the signal/idler count rate is 6.3 times larger than the coincidence count rate. When the photon energy of the signal is 13.5 keV, the signal count rate is higher than the coincidence count rate by a factor of 171.4.

At x-ray wavelengths Compton scattering of the pumping beam is significantly stronger than the down converted signal. Detection is therefore done by coincidence counting of the signal and idler photons. Typically, the main noise source is simultaneous Compton counts at the two detectors, and the noise is proportional to the square of the Compton scattering rate and to the square of the path length that the pump travels in the nonlinear crystal. The theory described here shows that only the last absorption length of the generating crystal contributes to the parametric coincidence count rate and any portion of the crystal longer than the absorption length contributes only to the background noise. The absorption length at 4.5 keV, which is the lowest photon energy we measure, is 0.108 mm. Our crystal length is 0.48 mm, and the optical path inside the crystal is 0.5 mm and 1.77 mm in transmission and reflection geometries respectively. By working in the transmission geometry, and not in reflection as in previous experiments, we obtain a ~ 12.5 improvement in the signal-to-noise ratio.

The Langevin method is a standard method to describe quantum systems that exhibit loss [11, 12]. Several authors have considered the effect of cavity output coupling and included the effect of Langevin terms on PDC [13–17]. The Langevin method has also been used to describe the generation of paired photons by electromagnetically induced transparency [18–22].

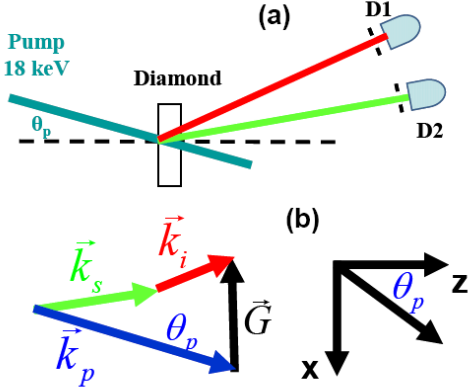


FIG. 1: (a) Schematic of the experiment. (b) Phase matching diagram. \vec{k}_s , \vec{k}_i , and \vec{k}_p are the wave vectors of the signal, idler, and pump fields. \vec{G} is the reciprocal lattice vector orthogonal to the (220) atomic planes.

A typical phase matching diagram for x-ray PDC is shown in Fig. 1. We denote the signal, idler, and pump wave-vectors respectively as \vec{k}_s , \vec{k}_i , and \vec{k}_p . \vec{G} denotes the reciprocal lattice vector. The phase matching condition is $\vec{k}_s + \vec{k}_i = \vec{k}_p + \vec{G}$. We use the (220) atomic planes with the lattice \mathbf{k} vectors in the direction of the x-axis. We develop the theory in the Heisenberg picture and define the transverse wave-vector $\mathbf{q}_j = (k_{jx}, k_{jy})$, where k_{jx} and k_{jy} are the wave-vector components parallel to the surfaces of the crystal. The output of the generator crystal is described by frequency domain operators $a_s(z = L, \mathbf{q}_s, \omega_s)$ and $a_i(z = L, \mathbf{q}_i, \omega_i)$, with $w_p = w_s + w_i$ and $\mathbf{q}_p + \mathbf{G} = \mathbf{q}_s + \mathbf{q}_i$. We consider a plane monochromatic pump at w_p propagating at an angle θ_p with regard to the z-axis in the x-z plane. The time-space signal and idler operators are related to their frequency domain counterparts by

$$a_s(z, \mathbf{r}, t) = \int_0^\infty \int_{-\infty}^\infty a_s(z, \mathbf{q}, \omega) \exp[-i(\mathbf{q} \cdot \mathbf{r} - \omega t)] d\mathbf{q} d\omega$$

$$a_i(z, \mathbf{r}, t) = \int_0^\infty \int_{-\infty}^\infty a_i(z, \mathbf{q}, \omega) \exp[-i(\mathbf{q} \cdot \mathbf{r} - \omega t)] d\mathbf{q} d\omega,$$

where $\mathbf{r} = (x, y)$, with commutators,

$$[a_j(z_1, \mathbf{q}_1, \omega_1), a_k^\dagger(z_2, \mathbf{q}_2, \omega_2)] = \frac{1}{(2\pi)^3} \delta_{j,k} \delta(z_1 - z_2) \delta(\mathbf{q}_1 - \mathbf{q}_2) \delta(\omega_1 - \omega_2). \quad (1)$$

The operators $a(z, \mathbf{q}, \omega)$ are the coarse grained annihilation operators of a photon in a specific mode. These operators are normalized so that the signal and idler count rate is $R_s = \langle a_s^\dagger(\mathbf{r}, t) a_s(\mathbf{r}, t) \rangle$ and $R_i = \langle a_i^\dagger(\mathbf{r}, t) a_i(\mathbf{r}, t) \rangle$

respectively. The factor $\delta_{j,k}$ is included in the commutator to account for the polarization property: When the pump polarization is normal to the scattering plane the polarization of the signal must be normal to the idler polarization [8].

We assume the slowly varying envelope equations by superposition of two physical effects, parametric down-conversion, and propagation in a lossy medium [12].

$$\frac{\partial a_s}{\partial z} + \frac{\alpha_s}{\cos \theta_s} a_s = \kappa' a_i^\dagger \exp[i\Delta k_z z] + \sqrt{\frac{2\alpha_s}{\cos \theta_s}} f_s,$$

$$\frac{\partial a_i^\dagger}{\partial z} + \frac{\alpha_i}{\cos \theta_i} a_i^\dagger = \kappa'^* a_s \exp[-i\Delta k_z z] + \sqrt{\frac{2\alpha_i}{\cos \theta_s}} f_i^\dagger. \quad (2)$$

The quantity $\Delta k_z = k_p \cos \theta_p - k_s \cos \theta_s - k_i \cos \theta_i$ is the phase mismatch in the direction normal to the diamond boundaries (along the z axis), where $k_j = \omega_j n(\omega_j)/c$. The boundary conditions impose exact phase matching in the x and y directions. In Eq. (2), θ_s and θ_i are the angles of the idler and the signal with respect to the surface normal and are found by solving the phase matching equations at the given pump angle and signal photon energy. The absorption coefficients as a function of the wavelength are α_s and α_i . $\kappa' = \frac{i\kappa}{\sqrt{\cos \theta_s \cos \theta_i}}$ where κ is the nonlinear coupling coefficient. The $f_s(z, \mathbf{q}, \omega)$ and $f_i^\dagger(z, \mathbf{q}, \omega)$ are the Langevin noise operators, and satisfy

$$[f_j(z, \mathbf{q}, \omega), f_k^\dagger(z', \mathbf{q}', \omega')] = \frac{1}{(2\pi)^3} \delta_{j,k} \delta(z - z') \delta(\mathbf{q} - \mathbf{q}') \delta(\omega - \omega'). \quad (3)$$

We solve Eq. (2) for the output operators $a_s(L, \mathbf{q}, \omega)$ and $a_i^\dagger(L, \mathbf{q}, \omega)$. These operators are expressed in terms of the vacuum fields at the input of the nonlinear generating crystal, $a_s(0, \mathbf{q}, \omega)$ and $a_i^\dagger(0, \mathbf{q}, \omega)$, integrals over the Langevin terms, and coefficients that depend on the signal frequency ω_s and the signal transverse \mathbf{k} vector \vec{q}_s . When loss is negligible, the contribution from the Langevin terms is negligible and the output operators can be written as a unitary transformation of the boundary operators. In this case, the commutators [Eq. (1)] are conserved at all z without the Langevin terms. We have shown numerically that when the loss cannot be ignored, the commutators are conserved at all z only when the Langevin terms are retained.

The coincidence count rate is

$$R_c = A \int \int G(\mathbf{u}, \tau) d\mathbf{u} d\tau,$$

where

$$G(\mathbf{u}, \tau) = \langle a_i^\dagger(\mathbf{r}_2, t_2) a_s^\dagger(\mathbf{r}_1, t_1) a_s(\mathbf{r}_1, t_1) a_i(\mathbf{r}_2, t_2) \rangle. \quad (4)$$

Here A is the area of the pump at the input of the nonlinear crystal, $\mathbf{u} = \mathbf{r}_2 - \mathbf{r}_1$ and $\tau = t_2 - t_1$.

The experiment described here was run at Beam-line 10-2 of SSRL. Fig. 1(a) depicts the experimental setup.

TABLE I: Angles of the detectors D1 and D2 with regard to the pumping beam. The pump is at an angle of 15.8853 degrees with regard to the surface normal; ω_s and ω_{s0} are the signal photon frequency and the degenerate photon frequency, respectively. Angles are in degrees.

ω_s/ω_{s0}	D1	D2
1	30.2837	33.104
1.1	30.4198	33.2804
1.2	30.5457	33.4493
1.3	30.6642	33.644
1.4	30.778	33.8753
1.5	30.8895	34.1604

The pump beam with a photon energy of 18 keV impinges on a diamond crystal. The pump flux was 2×10^{11} photons/s. The crystal length is 0.48 mm and the spot size at the sample was 1.2×10^{-7} m². The polarization of the pump is normal to the scattering plane. The idler and signal beams are detected on two separate detectors with variable apertures D1 and D2. A helium bag between the output of the diamond and the slits of the detectors reduced the loss due to air absorption. The angle of the surface normal of the diamond crystal relative to the k vector of the pump beam is 15.8853 degrees. The various angles of the detectors relative to the pump pointing are given in Table I. To determine the coincidence count rate, we scan through the recorded data and count events that satisfy the following conditions: (1) the photon energy at detector D2 is within a certain energy acceptance window and (2) both detectors record a count within a time window smaller than the electronic response time. In order to build energy histograms, we constrain the counts at detector D2 to be in a fixed energy window, and we do not constrain the photon energies at detector D1.

Typical energy histograms of the coincidence count rate generated via the PDC process are shown in Fig. 2. Here, panels (a) and (b) correspond to detector angles satisfying off-degeneracy phase matching energy ratios of $\omega_s/\omega_{s0} = 1.2$ and $\omega_s/\omega_{s0} = 1.3$, respectively.

Both theory and the experimental results of Fig. 2 show that the energy of the down converted photons correspond to a particular emission angle. This one-to-one relation between photon energy and the emission angle is determined by phase matching. Theory also predicts that the total width of the angular distribution of the photon pairs emerging from the crystal is larger than that of the apertures of the detectors. Therefore, the width of the observed energy distribution is limited by the angular acceptance of the detector apertures.

The measured coincidence count rate depends on the choice of the energy window for detector D2 and on the aperture sizes of both D1 and D2. For equal angular acceptances, we plot the energy histograms similar to Fig. 2 for an energy window from 0.1 keV to 1.3 keV. We repeat this for each of the detector angles in Table I. We sum

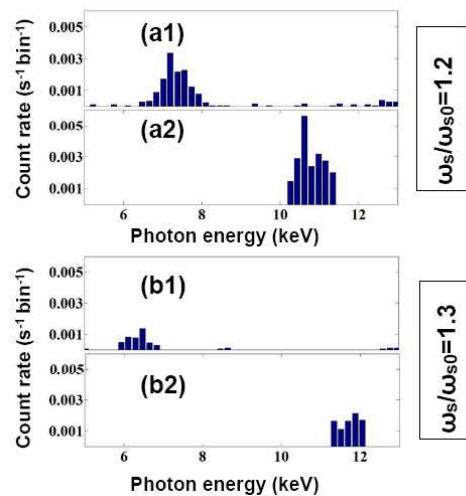


FIG. 2: Energy histograms of the coincidence count rate at (a) $\omega_s/\omega_{s0} = 1.2$ off of degeneracy and (b) $\omega_s/\omega_{s0} = 1.3$ off of degeneracy. Parts (a1) and (b1) are the energy histograms of detector D1. Parts (a2) and (b2) are the energy histograms of detector D2. The events displayed satisfy the conditions: (1) The photon energy at D2 is within an energy window of 0.8 keV in part (a2) and 0.6 keV in part (b2). (2) Both detectors "click" within a time window which is smaller than the system response time. The photon energy of the pump is 18 keV

over the D1 counts and scale for detector efficiencies and propagation losses (helium bag and the air gap between the slits and the detectors). We repeat this procedure for unequal angular acceptances (a ratio of 3.6 between solid angles of the detectors; see supplemental material) case for an energy window from 0.1 keV to 1 keV. Fig. 3 shows the total coincidence count rate as a function of the energy window. The first row shows the degeneracy phase-matching case $\omega_s/\omega_{s0} = 1$, the second row the off-degeneracy case $\omega_s/\omega_{s0} = 1.3$. The first column shows the equal angular acceptance case ($\Omega_1 = \Omega_2$), while the second column shows the $\Omega_1 = 3.6 \cdot \Omega_2$ case.

Figure 4 shows total coincidence count rate as a function of the deviation from the degenerate frequency. In part (a) the aperture sizes are equal and in part (b) the aperture size of detector D1 is larger than the aperture size of detector D2 by a factor of 3.6. The theoretical curve is scaled vertically by a common factor of 0.43. As we see from Fig. 4, the theoretical curves and the experimental results are in reasonable agreement.

The maximum generated pair rate at the degenerate frequency is one photon pair per 40 seconds. This observed count rate together with the theoretical calculation of the nonlinearity for signal polarization in and out of the scattering plane, yield $(\kappa L)^2 = 5 \times 10^{-25}$ for either polarization.

In summary, we have described the measurement of the coincidence count rates of photon pairs generated via x-

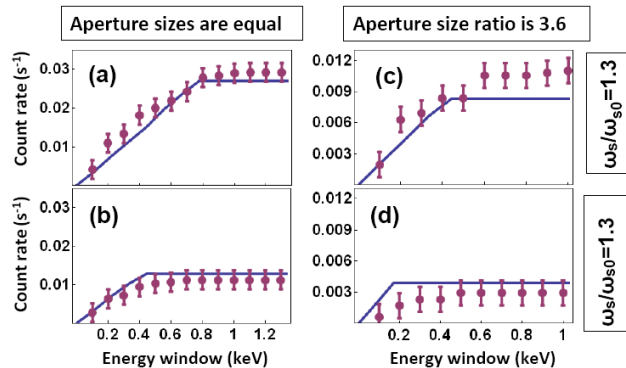


FIG. 3: Coincidence count rate vs. energy window at (a),(c) at degeneracy and (b),(d) at $\omega_s/\omega_{s0} = 1.3$. In parts (a) and (b) the aperture sizes are equal. In parts (c) and (d) the aperture size ratio is 3.6. Each of the points is a sum over the corresponding coincidence histogram as shown in Fig. 2. The solid blue curves are plotted from theory. The theoretical curves are scaled vertically by a factor of 0.43.

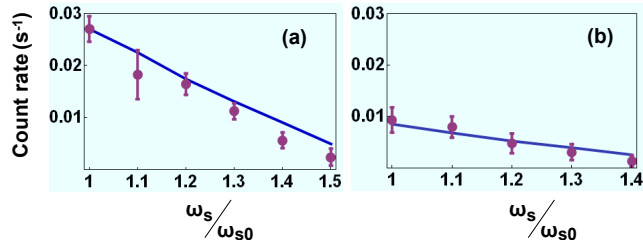


FIG. 4: Coincidence count rate as a function of ω_s/ω_{s0} . The solid blue curves are plotted from theory. The theoretical curves are scaled vertically by a factor of 0.43. (a) Aperture sizes are equal. (b) The aperture size ratio is 3.6.

ray PDC on, and off, of degeneracy. These measurements were possible due to the improvement in the signal-to-noise ratio achieved by working in the transmission geometry. We have described the theory of coincidence count rate in the presence of loss and showed that the Langevin terms are essential. The Heisenberg-Langevin equation (Eq. (2)) is based on the fluctuation-dissipation theorem with the assumption of a Markovian reservoir. Microscopically, to the extent that the loss is dominated by photoionization, the fluctuation may be viewed as resulting from (virtual) two body recombination. If there is loss but no parametric coupling, then two body recombination does not result in photon generation at either the signal or the idler. But in the presence of parametric coupling, recombination at the idler causes generation of signal photons, and recombination at the idler causes generation of signal photons.

The authors thank Yaron Silberberg for helpful discussions and for suggesting the data analysis procedure.

We thank Ron Shen for useful discussions. We acknowledge the help of Adi Natan, Alan Miahnahri, Mike Toney, and Bill White with the experimental setup and procedures. We thank Bart Johnson and Valery Borzenets for their assistance with the x-ray diffraction setup. Portions of this research were carried out at the Stanford Synchrotron Radiation Light source, a national user facility operated by Stanford University on behalf of the U.S. Department of Energy, Office of Basic Energy Sciences. This work was supported by the U.S. Air Force Office of Scientific Research and the U.S. Army Research Office. RNC is supported by the U.S. Department of Energy, Office of Basic Energy Sciences.

* E-mail me at: shwartz@stanford.edu

- [1] D. Bouwmeester, A. Ekert, A. Zeilinger, *The Physics of Quantum Information: Quantum Cryptography, Quantum Teleportation, and Quantum Computation*, Springer, New York, 2000.
- [2] I. Freund and B. F. Levine, *Phys. Rev. Lett.* **23**, 854857 (1969).
- [3] P. M. Eisenberger and S. L. McCall, *Phys. Rev. Lett.* **26**, 684-688 (1971).
- [4] B. W. Adams, *Nonlinear Optics, Quantum Optics, and Ultrafast Phenomena with X-Rays*. Kluwer Academic Publisher, (2008).
- [5] K. Tamasaku, and T. Ishikawa, *Phys. Rev. Lett.* **98**, 244801 (2007).
- [6] K. Tamasaku, K. Sawada, and T. Ishikawa, *Phys. Rev. Lett.* **103**, 254801 (2009).
- [7] K. Tamasaku, K. Sawada, E. Nishibori, and T. Ishikawa, *Phys. Rev. Lett.* **7**, 705-708 (2011).
- [8] S. Shwartz and S. E. Harris, *Phys. Rev. Lett.* **106**, 080501 (2011).
- [9] R. L. Byer and S. E. Harris, *Phys. Rev.* **168**, 1064 (1968).
- [10] D. A. Kleinman *Phys. Rev.* **174**, 1027 (1968).
- [11] M. O. Scully and M. S. Zubairy, *Quantum Optics*, Cambridge University Press, (1997).
- [12] Y. Yamamoto and A. Imamoglu, *Mesoscopic quantum optics*, John Wiley & Son Inc, New York (1999).
- [13] Zhang Tian-Cai, Xie Chang-De, and Pengkum-Chi, *Acta Physica Sinica* **1**, 94 (1992).
- [14] C. Simon and D. Bouwmeester, *Phys. Rev. Lett.* **91**, 053601-1(2003).
- [15] Sintayehu Tesfa, *Eur. Phys. J. D* **46**, 351358 (2008).
- [16] J. Perina and J. Krepelka, *Opt. Commun.* **282**, 3918 (2009).
- [17] Domenico Cuozzo and Gian-Luca Oppo, *Phys. Rev. A* **84**, 043810 (2011).
- [18] V. Balic, et al. *Phys. Rev. Lett.* **94**, 183601 (2005).
- [19] P. Kolchin, *Phys. Rev. A* **75**, 033814 (2007).
- [20] C. H. Raymond Ooi, Q. Sun, M. S. Zubairy, and M. O. Scully, *Phys. Rev. A* **75**, 013820 (2007).
- [21] C. H. Raymond Ooi and M. O. Scully, *Phys. Rev. A* **76**, 043822 (2007).
- [22] D. Shengwang, W. Jianming, and H. R. Morton, *J. Opt. Soc. Am. B* **25**, c98 (2008).